Potential Mechanisms of Intraocular Pressure Reduction by Micropulse Transscleral Cyclophotocoagulation in Rabbit Eyes

Hotaka Nemoto,[1] Megumi Honjo,[1] Michiaki Okamoto,[2] Koichiro Sugimoto,[1] and Makoto Aihara[1]

[1]Department of Ophthalmology, Graduate School of Medicine, The University of Tokyo, Tokyo, Japan
[2]Tomey Corporation, Nagoya, Japan

Correspondence: Megumi Honjo, Department of Ophthalmology, University of Tokyo School of Medicine, 7-3-1 Hongo Bunkyo-ku, Tokyo 113-8655, Japan; honjomegumi@gmail.com.

Received: February 8, 2022
Accepted: May 14, 2022
Published: June 2, 2022

Citation: Nemoto H, Honjo M, Okamoto M, Sugimoto K, Aihara M. Potential mechanisms of intraocular pressure reduction by micropulse transscleral cyclophotocoagulation in rabbit eyes. *Invest Ophthalmol Vis Sci.* 2022;63(6):3. https://doi.org/10.1167/iovs.63.6.3

Purpose. To evaluate the histological changes associated with, and the potential mechanisms of, intraocular pressure (IOP) reduction by micropulse cyclophotocoagulation (MP-CPC) in rabbit eyes.

Methods. MP-CPC was performed on the right eyes of Dutch belted rabbits, whereas the left eyes served as controls. The laser power settings were 250, 500, 750, 1000, 1500, and 2000 mW, 10 seconds per sweep, 100 seconds in total. IOP, outflow facility, and uveoscleral outflow tract imaging, using a fluorescent tracer, were examined at one week after MP-CPC. Changes of morphology and protein expressions in the outflow tissues, conjunctiva, and sclera were also evaluated.

Results. Significant reductions in IOP after MP-CPC were observed at 500 to 1000 mW ($P = 0.036$ and $P = 0.014$, respectively). The pre-MP-CPC IOP was 11.35 ± 0.41 mm Hg. At one week after surgery, the respective IOP values in the eyes treated at 500 mW and 1000 mW were 9.45 ± 0.49 mm Hg and 7.4 ± 0.27 mm Hg, respectively. Severe ciliary body damage was observed at 1500 to 2000 mW. MMP1–3 and fibronectin expression levels in the outflow tract and ciliary body were upregulated after MP-CPC. The α-smooth muscle actin (α-SMA) was upregulated at higher power levels. MP-CPC significantly increased uveoscleral outflow, whereas the outflow facility did not change. The α-SMA, collagen, and fibronectin were significantly upregulated in the subconjunctiva and sclera.

Conclusions. Reactive fibrotic responses were observed in the outflow tract, conjunctiva, and sclera after MP-CPC. A potential mechanism of IOP reduction by MP-CPC in pigmented rabbit eyes may involve increased uveoscleral outflow related to MMP upregulation.

Keywords: micropulse transscleral cyclophotocoagulation, intraocular pressure, ciliary body, matrix metalloprotease, uveoscleral outflow

Glaucoma is a disease that causes progressive visual field defects and irreversible visual impairment.[1,2] Intraocular pressure (IOP)–lowering therapy has been shown to prevent progression of visual field defects.[3–5] Continuous-wave cyclophotocoagulation (CW-CPC) is widely used to lower IOP by suppressing aqueous humor production through cyclo-destruction of the ciliary process.[6,7] However, use of CW-CPC is limited to severe cases because of adverse effects such as severe postoperative intraocular inflammation, decreased vision, scleral melt, hypotony, and phthisis bulbi.[8]

The recently developed micropulse cyclophotocoagulation (MP-CPC) technique, which uses micropulse diode laser photocoagulation at a wavelength of 810 nm (Cyclo G6TM; Iridex Corporation, Mountain View, CA, USA) and MP3 probes, has rapidly gained popularity because it causes fewer complications.[9,10] CW-CPC generally targets pigmented tissues up to the photocoagulative threshold. In contrast, micropulse mode administers a series of short diode-laser pulses, separated by pauses that theoretically allow tissues to cool.[11,12] Therefore micropulse mode is presumed to minimize collateral tissue damage.[13] MP-CPC is reportedly safer, with fewer complications in both advanced refractory glaucoma and in earlier stages of glaucoma, sometimes even before the use of glaucoma filtration surgery.[9,10,14,15] Optical coherence tomography images after MP-CPC have revealed increased choroidal thickness, and increased space between ciliary muscle bundles has also been reported; the resultant increase in uveoscleral outflow has been proposed as a mechanism for IOP reduction.[16–18] However, many unanswered questions regarding this mechanism remain, such as how MP-CPC increases uveoscleral outflow without obvious tissue destruction.

In the present study, we explored the optimal laser power to lower IOP without severe tissue damage; we confirmed that MP-CPC at optimal power lowers IOP and increases

uveoscleral outflow in rabbit eyes. We also explored the possible mechanisms of IOP reduction and tissue changes in rabbit eyes after MP-CPC.

Materials and Methods

Animals

This study was performed in accordance with the ARVO Statement for the Use of Animals in Ophthalmic and Vision Research, and was approved by the Institutional Animal Research Committee of the University of Tokyo. Thirty female Dutch belted rabbits (1.5–1.99 kg, 14–19 weeks old; Kitayama Labes Co., Ltd., Nagano, Japan) were used in this study. All rabbits were acclimatized for seven days before experiments began; they were kept in a conventional animal room with appropriately controlled temperature and humidity (22° ± 3°C and 55% ± 10%, respectively), and a 12-hour light/dark cycle. The rabbits were provided tap water and food as desired.

Micropulse Cyclophotocoagulation

In total, 30 right rabbit eyes were treated with MP-CPC, and sham surgeries were performed on the left eyes as controls. MP-CPC was performed with the rabbits under sedation using intramuscular ketamine (40 mg/kg) and xylazine (5 mg/kg), as well as topical (oxybuprocaine hydrochloride 0.4%) anesthesia. MP-CPC was performed using a Cyclo G6 Glaucoma Laser system with a MicroPulse P3 Glaucoma device (Iridex Laser Systems, Mountain View, CA, USA), and Cycloprobe Rev2. The laser power was adjusted to 250, 500, 750, 1000, 1500, or 2000 mW; an 810-nm infrared diode laser was used with a 31.3% duty cycle for 50 seconds superiorly and 50 seconds inferiorly (total: 100 seconds). Hydroxyethyl cellulose drops (Scopisol Solution For Eyes; Senju Pharmaceutical Co., Ltd., Osaka, Japan) were applied, and the front edge of the cycloprobe was placed at the limbus. The procedure was performed with the laser directed toward the pars plana. The areas at 3 o'clock and 9 o'clock, where the ciliary neurovascular bundle is located, were avoided; laser irradiation was performed in a back-and-forth manner for 10 seconds per pass. The sham procedure was performed without laser irradiation. After surgery, topical betamethasone sodium phosphate 0.1% eye drops were applied to both eyes twice daily for one week. The power output was confirmed using a power meter at the beginning and end of the study.

IOP Measurement and Outflow Evaluation

IOP was measured using TonoVet (M.E. Technica, Tokyo, Japan) under topical anesthesia. Aqueous humor outflow was measured using the two-level constant pressure infusion method, as previously reported.[19] Under sedation with intramuscular ketamine and xylazine, together with topical anesthesia, the eyes were cannulated using a 32-G sharp needle connected to a polyethylene tube with an inner diameter of 1.0 mm. A reservoir bag was connected to the other end of the tube. The height of the reservoir bag was changed to adjust the IOP to 15 mm Hg; the flow volume (Fc_1) through the tube lumen was measured for 10 minutes. The height of the reservoir bag was then changed to an IOP of 20 mm Hg, and the flow volume (Fc_2) was again measured for 10 minutes. The Goldmann equation was used to calculate the outflow facility (C), as follows:

$$C = (Fc_1 - Fc_2)/50.$$

Tracer Preparation

To determine the uveoscleral outflow, we used 70-kDa dextran conjugated to tetramethyl-rhodamine, which has been used as a tracer in mice.[20] Dextran was dissolved in phosphate-buffered saline solution to prepare a stock solution with a concentration of 2 mg/mL. The stock solution was spun in a centrifuge at 1200 rpm for 20 minutes and then sterilized by filtration through a 0.22-µm pore filter (Millipore, Burlington, MA, USA). The stock solution was diluted tenfold in phosphate-buffered saline solution and used for the experiments.

Tracer Injection

Tetramethyl-rhodamine-conjugated 70-kDa dextran solution was used to fill a 1-mL syringe connect to a 30-G sharp needle. The needle was inserted into the cornea, and 0.05 mL of the solution was administered into the anterior chamber. The needle was then quickly removed, and absence of corneal leakage was confirmed. Twenty minutes after administration, the rabbits were euthanized using intravenous secobarbital sodium (100 mg/kg), and the eyes were enucleated for histological evaluation.

Histology and Immunofluorescence

After enucleation, incisions were made in the cornea and sclera; the eyes were immediately immersed in 4% paraformaldehyde and fixed for 24 hours. They were then dehydrated with 30% sucrose for 12 hours, cut in half, and embedded in optimal cutting temperature compound (Tissue-Tek; Sakura Fine Technical, Tokyo, Japan) to make 10-µm frozen sections. Immunofluorescence staining experiments were performed as described previously.[21] The frozen sections were incubated overnight at 4°C with the following primary antibodies: collagen type I (ab6308, 1:500; Abcam, Cambridge, UK), a-smooth muscle actin (α-SMA) (ab21027, 1:500; Abcam), fibronectin (ab6328, 1:500; Abcam), matrix metalloproteinase-1 (MMP-1) (12011-01, 1:500; Southern Biotech, Birmingham, UK), matrix metalloproteinase-2 (MMP-2) (F-68, 1:500; Kyowa Pharma Chemical Co., Toyama, Japan), and matrix metalloproteinase-3 (MMP-3) (F-77, 1:500; Kyowa Pharma Chemical Co.). The secondary antibodies were goat anti-mouse Alexa-647 (4410S, 1:1000; Cell Signaling Technology, Danvers, MA, USA) and donkey anti-goat Alexa-633 (A21082, 1:1000; ThermoFisher, St. Louis, MO, USA). Nuclei were stained with 4′,6-diamidine-2-phenylindole dihydrochloride solution (4 µg/mL; Fujifilm Wako Pure Chemical, Osaka, Japan). To evaluate the uveoscleral outflow tract, frozen sections of eyes with tetramethyl-rhodamine–labeled dextran in the anterior chamber were used to prepare slides. Images were obtained using a confocal microscope (LSM880 with Airyscan; Carl Zeiss, Oberkochen, Germany). The researcher who analyzed the data was blinded to the treatment. The fluorescence intensity was determined by measuring the signal intensity of the ciliary body in the region of interest, and analyzed using ImageJ software (http://imagej.nih.gov/ij/; National Institutes of Health, Bethesda, MD, USA). Nonspe-

Investigative Ophthalmology & Visual Science

cific signals, such as autofluorescence or background staining, were identified by using a negative control sample, and contrast adjustment was used to hide the nonspecific signals. Among the tracer signals in the uveoscleral tract, the length of the straight-line distance from the trabecular meshwork to the most distal signal was measured using image J. Normalization was performed by dividing the intensity obtained at each laser power by the average of the control signal intensities. Three images from three rabbit eyes were analyzed for each power; the relative changes in area and fluorescence of each group are presented using bar graphs.

Western Blotting

Rabbit eyes were enucleated one week after laser. The ciliary bodies were obtained, rinsed with saline solution, then collected in RIPA buffer (Thermo Fisher Scientific K.K., Kanagawa, Japan) containing protease inhibitor (Roche Diagnostics, Basel, Switzerland), left on ice for 30 minutes before homogenization, stored at −80°C overnight, and spun in a centrifuge the next day, and the supernatant was collected. Protein concentration was measured by bicinchoninic acid assay using BCA Protein Assay Kit (Thermo Fisher Scientific, Waltham, MA, USA). Western blotting (WB) was performed as previously described.[21] Protein bands were detected by ImageQuant LAS 4000 mini (GE Healthcare, Chicago, IL, USA). Primary antibodies were anti-fibronectin (ab6328, 1:5000; Abcam), α-SMA (ab21027, 1:5000; Abcam), MMP-1 (12011-01, 1:5000; Southern Biotech, Birmingham, UK), MMP-2 (F-68, 1:5000; Kyowa Pharma Chemical Co., Toyama, Japan), and MMP-3 (F-77, 1:5000; Kyowa Pharma Chemical Co.). Horseradish peroxidase–conjugated secondary antibody (1:5000) was purchased from Thermo Fisher Scientific (goat anti-mouse IgG), and Santa Cruz Biotechnology (Dallas, TX, USA; rabbit anti-goat IgG). The β-actin served as the loading control. All membranes were stripped of antibodies using WB Stripping solution and then incubated with mouse monoclonal antibody β-actin (1:10000) and subsequently with horseradish peroxidase–conjugated antibody (1:5000). Densitometry of scanned films was performed using ImageJ; protein expression levels are expressed relative to the level of β-actin.

Statistical Analysis

The data were statistically analyzed using Microsoft Excel version 2016 statistical analysis tool (Redmond, WA, USA). The results are expressed as means ± standard errors of the mean. Differences among groups were analyzed using one-way analysis of variance, followed by Welch's t test. A P value <0.05 was considered statistically significant.

Results

IOP Decrease and Change in Outflow Facility After MP-CPC

We examined the presence of tissue changes, IOP, and outflow facility in rabbits after MP-CPC. At laser powers below 1000 mW, there were no significant structural changes or tissue damage to the ciliary body, sclera, or ciliary muscles (Fig. 1A). At laser powers of 1500 to 2000 mW, a distinct "pop" sound was heard during the laser treatment; hematoxylin-eosin–stained tissue sections showed structural changes, such as ciliary thickening, hemorrhage, and pigment dispersion within the ciliary body at 2000 mW, whereas mild hemorrhage was present within the ciliary body at 1500 mW (Fig. 1A). Therefore we considered the adequate MP-CPC power for rabbit eyes to lower IOP without causing tissue damage to be less than 1000 mW.

MP-CPC in rabbit eyes at 250 mW did not show significant IOP reduction (after three days: $P = 0.356$, after seven days: $P = 0.415$, respectively), whereas 500 to 1000 mW resulted in significant IOP reduction after three ($P = 0.019$, $P = 0.006$, respectively) and seven days ($P = 0.036$, $P = 0.014$, respectively) (Fig. 1B). However, outflow facility did not change significantly after MP-CPC ($P = 0.477$ and $P = 0.312$ for 500 and 1000 mW, respectively) (Fig. 1C), implying that MP-CPC does not enhance the conventional outflow.

Uveoscleral Outflow Tract Imaging Using a Fluorescent Tracer

To elucidate the mechanism by which MP-CPC lowers IOP in rabbit eyes, we examined the uveoscleral outflow tract by imaging a fluorescent tracer. We found that MP-CPC increased uveoscleral outflow (Fig. 2A). At one week after MP-CPC, tracer outflow was limited to the trabecular meshwork without laser treatment after 20 minutes of tracer administration; no signal was observed in the uveoscleral outflow tract. Distinct tracer signals were observed in the uveoscleral outflow tract at 500 and 1000 mW. Furthermore, although there were no statistically significant differences, both tracer length and ciliary signal intensity tended to be greater at 1000 than at 500 mW, implying that MP-CPC enhanced uveoscleral outflow in a power-dependent manner (Figs. 2B, 2C).

MMP Expression Patterns in the Ciliary Body After MP-CPC

To elucidate the mechanism by which MP-CPC increases uveoscleral outflow, we used immunostaining to evaluate the expression patterns of MMP1–3 in the ciliary body after MP-CPC. Although MMP1 expression was observed in the ciliary epithelium with laser treatments as low as 250 mW, significant upregulation of MMP1 was observed at powers higher than 1000 mW (Figs. 3A, 3B, 3C). Upregulation of MMP2 expression was evident at 250 to 2000 mW, localized in the area between the ciliary muscle bundles (Fig. 4A). MMP2 upregulation increased with the power; it was statistically significant at 250, 1000, 1500, and 2000 mW (Figs. 4B, 4C). MMP3 upregulation was observed from 250 mW; it was statistically significant at 1000, 1500, and 2000 mW (Figs. 5A, 5B, 5C). MMP3 expression was also upregulated in response to the power (Figs. 5B, 5C). Notably, the increased expression levels of MMP1–3 were localized in the area between the ciliary muscle bundles, known as the uveoscleral outflow tract; they were most strongly localized at the scleral junction.

Changes in the Expression Patterns of Fibrotic Markers in the Ciliary Body

We then investigated changes in the expression patterns of fibrotic markers in response to MP-CPC. The α-SMA expression in the ciliary muscle qualitatively increased in all MP-CPC groups, compared to controls (Fig. 6A). Furthermore, increased α-SMA expression was observed from

Investigative Ophthalmology & Visual Science

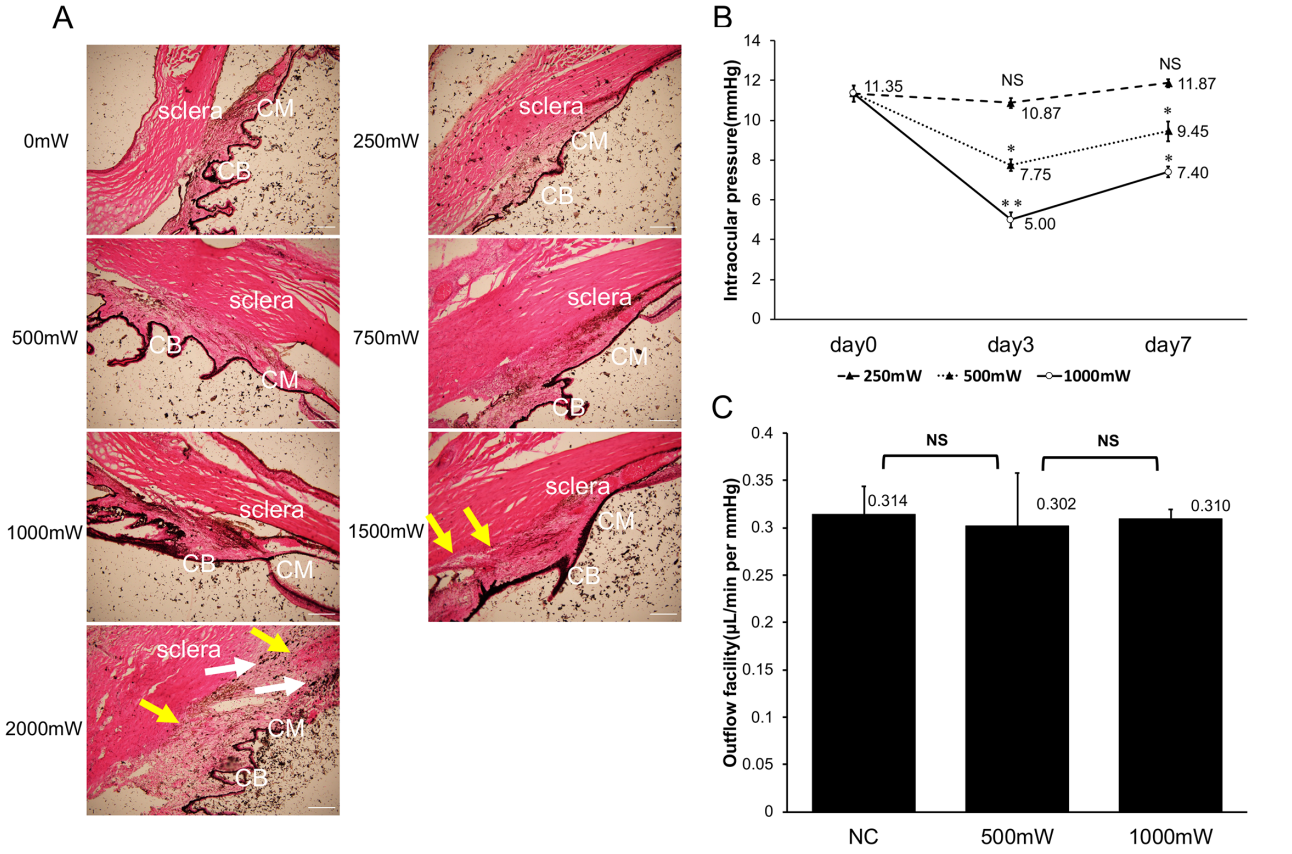

Figure 1. Histological sections, IOP, and outflow facility after MP-CPC. (**A**) Microscopic images of hematoxylin-eosin–stained tissue sections one week after MP-CPC. At laser powers below 1000 mW, there were no significant structural changes or tissue damage to the ciliary body, sclera, or ciliary muscles. Mild hemorrhage was present within the ciliary body at 1500 mW. At 2000 mW, ciliary thickening, hemorrhage, and pigment dispersion within the ciliary body were observed. The *white* and *yellow arrows* point to pigment dispersion and hemorrhage, respectively. *Scale bar*: 200 µm. (**B**) IOP before and at three and seven days after MP-CPC at 500 mW and 1000 mW, respectively (n = 3). Both 500 mW and 1000 mW resulted in significant IOP reduction after three and seven days. (*C*) Outflow facility before and at seven days after MP-CPC at 500 mW and 1000 mW, respectively (n = 3). Outflow facility did not change significantly after MP-CPC. $^{*}P < 0.05$, $^{**}P < 0.01$. Data are presented as means ± standard errors of the mean, Welch's *t* test.

250 to 2000 mW, coinciding with the ciliary muscle bundles, but the signal strength was stable only at laser powers above 250 mW. Although fluorescence intensity increased and the area stained with α-SMA showed broad fluorescence signals beyond the ciliary muscle bundles up to the sclera, the difference was not statistically significant because of large variance between groups (Figs. 6B, 6C).

In contrast, fibronectin showed a diffusely spreading and increasing fluorescence signal within the ciliary muscle bundles in response to increased laser power (Figs. 7A, 7B, 7C). Fibronectin upregulation was statistically significant at all laser powers higher than 250 mW.

Assessment by WB of Fibronectin, α-SMA, and MMP1-3 Expression in Ciliary Body After MP-CPC

To validate the protein expression patterns obtained by immunostaining, semiquantitative analysis of proteins in the ciliary body was performed by WB (Fig. 8). Similar to the immunostaining results, fibronectin expression in the ciliary body increased with laser power, with statistically significant differences at 500 mW, 750 mW, 1500 mW, and 2000 mW (Fig. 8B). The α-SMA showed no statistically significant differences in immunostaining, but WB showed statistically significant differences at 1000 mW and 2000 mW (Fig. 8C). Similar to the immunostaining results, MMP1 also showed an increase in expression in response to laser power, with a statistically significant difference at 2000 mW (Fig. 8D). Statistically significant differences were observed for MMP2 at 1500 mW and 2000 mW, and for MMP3 at 500 mW, 750 mW, 1000 mW, and 2000 mW, respectively (Figs. 8E, 8F).

Changes in the Expression Patterns of Fibrotic Markers in the Conjunctiva and Sclera

We also investigated changes in the expression patterns of fibrotic markers in the laser-treated conjunctiva and sclera (Figs. 9A, 9B, 9C). An increase in α-SMA positive cells was observed beginning at 500 mW; the signals increased in response to increasing laser power, implying that subconjunctival myofibroblasts may be recruited to produce collagen (Fig. 9A). The expression patterns of collagen type I and fibronectin also changed in response to increased laser power in the subconjunctival region (Figs. 9B, 9C).

Investigative Ophthalmology & Visual Science

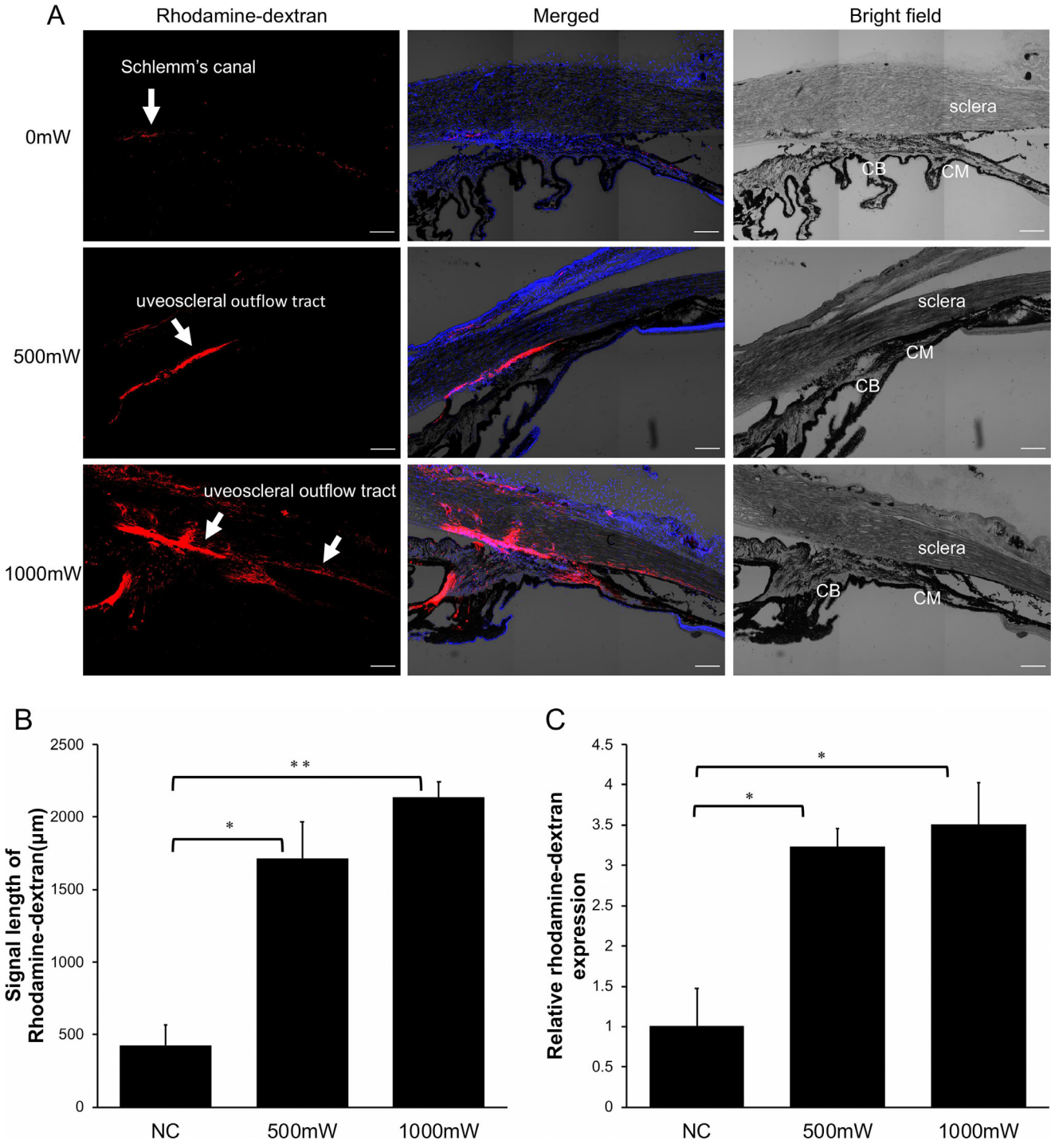

Figure 2. Uveoscleral outflow tract imaging and graphs of intensity analysis using a fluorescent tracer. (**A**) The *left panels* show images of the fluorescent tracer, the *right panels* show bright field, and the *middle panels* show merged images of fluorescent tracer, DAPI, and bright field. The tracer signal was observed in a more posterior area of the uveoscleral outflow tract at 1000 than at 500 mW. *Scale bar*: 200 µm. (**B**) Graph of the fluorescent tracer signal length obtained on the uveoscleral outflow tract from the trabecular meshwork (n = 3). (**C**) Graph of signal intensity of fluorescent tracer in the ciliary body (n = 3). Data are presented as means ± standard errors of the mean, Welch's *t* test. $^{*}P < 0.05$, $^{**}P < 0.01$.

Upregulation of collagen type I was observed in both the subconjunctival area and the sclera, particularly at laser powers higher than 1000 mW (Fig. 9B); these findings indicate the formation of short and tortuous collagen fibers after MP-CPC, which differed from the long and well-defined scleral fibers. Reactive upregulation of fibronectin was significant at laser powers higher than 750 mW (Fig. 9C).

Investigative Ophthalmology & Visual Science

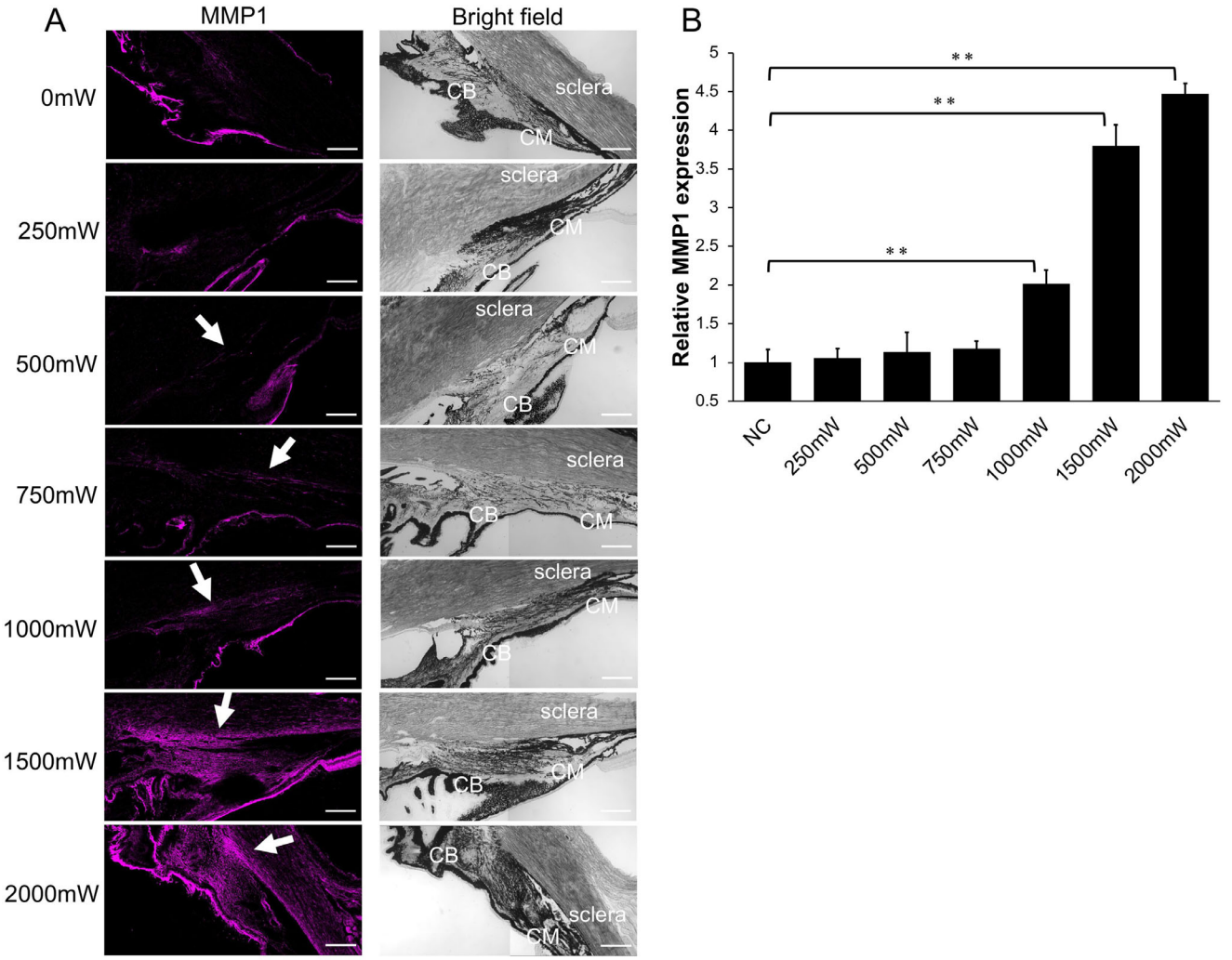

Figure 3. Immunofluorescence staining images and graphs of MMP1 expression patterns. (**A**) The *left panels* show images that were stained with MMP1, the *right panels* show bright field. Significant upregulation of MMP1 was observed in response to increased laser power, localized in the area between the ciliary muscle bundles. The *white arrows* point to areas of MMP1 upregulation. *Scale bar*: 200 µm. (**B**) A graph of the fluorescence intensity of ciliary body. Data are presented as means ± standard errors of the mean (n = 3), Welch's *t* test. $^{*}P < 0.05$, $^{**}P < 0.01$.

Discussion

Clinical studies have demonstrated that MP-CPC effectively lowers IOP, in a manner comparable to CW-CPC, with a superior safety profile and without severe complications.[9,15,22] Increased uveoscleral outflow is presumably one of the mechanisms by which MP-CPC lowers IOP; this hypothesis is based on pathological evidence of increased space among ciliary muscle bundles and clinical optical coherence tomography findings of increased choroidal thickness in human eyes.[16–18] Furthermore, the effects and complications of MP-CPC are suspected to vary depending on the energy level applied.[23] However, precise changes in outflow tissues and the underlying mechanisms have not been described. In the present study, we collected novel data that imply an increased uveoscleral outflow after MP-CPC, as well as MMP upregulation in the uveoscleral outflow tract.

Previous studies have reported that another potential mechanism of IOP reduction after MP-CPC in pigmented rabbits could be aqueous humor transport dysfunction caused by damage to the nonpigmented epithelial cells of the pars plicata, a mechanism similar to CW-CPC.[12,24,25] Additionally, inflammation and scarring in the ciliary body in MP-CPC and CW-CPC are reportedly similar. Although aqueous humor transport dysfunction could be a mechanism for the IOP-lowering effects of MP-CPC, damage to the ciliary body may be reversible and cannot explain the long-term IOP-lowering effects. In addition, previous studies used the laser power levels that are usually applied in humans. The results cannot be applied to rabbit eyes because rabbit tissues are more vulnerable than human tissues, because of substantial interspecies anatomical differences. Therefore it is important to use suitable laser power levels in rabbits when exploring the IOP-lowering effects of MP-CPC. In this study, we explored the optimal laser power for IOP reduction without severe tissue damage; we demonstrated that MP-CPC at an optimal power level effectively lowered IOP in rabbit eyes. We also found severe damage to the ciliary body and reactive fibrotic responses both in the outflow tract and the ciliary body at higher laser powers; such

Investigative Ophthalmology & Visual Science

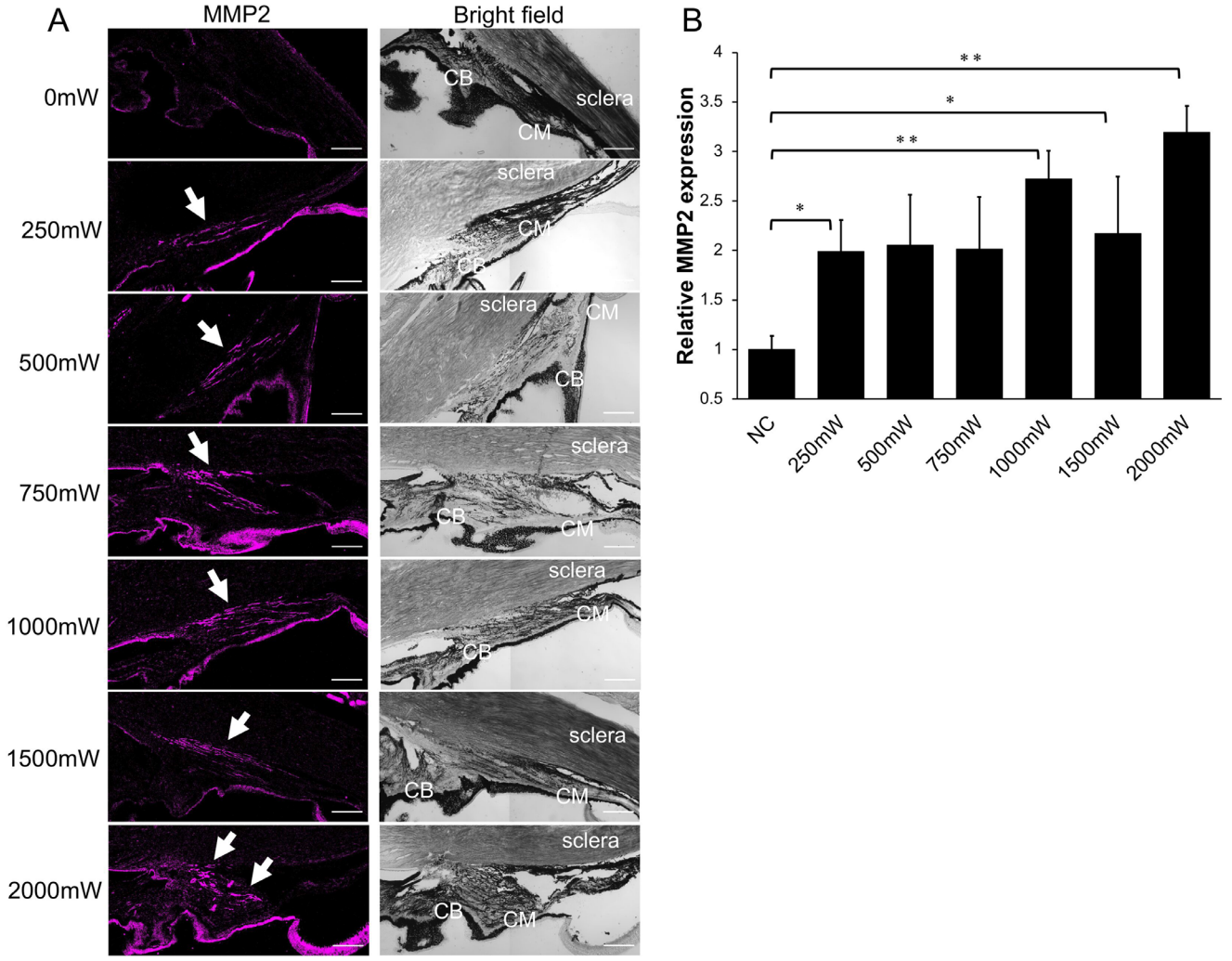

Figure 4. Immunofluorescence staining images and graphs of MMP2 expression patterns. (**A**) The *left panels* show images that were stained with MMP2, the *right panels* show bright field. Significant upregulation of MMP2 was observed in response to increased laser power, localized in the area between the ciliary muscle bundles. The white arrows point to areas of MMP2 upregulation. *Scale bar*: 200 µm. (**B**) A graph of the fluorescence intensity of ciliary body. Data are presented as means ± standard errors of the mean ($n = 3$), Welch's t test. $^{*}P < 0.05$, $^{**}P < 0.01$.

findings were minimized when using the appropriate laser power.

Initially, we verified which laser power could reduce IOP in a manner comparable to the clinical data available for humans, without irreversible degeneration caused by thermal coagulation. In the present study, we chose the ablation protocol with 100 seconds in total, which was the standard developer's recommendation when we started the experiment with the newly developed Rev2 probe. The ablation time of 160 seconds in total has become popular in clinical practice; our results in rabbit eyes in the present study are consistent and comparable to the mechanisms of MP-CPC in the clinical practice, because we have determined the appropriate laser power that can lower intraocular pressure without tissue destruction similar to human ocular tissue. Although a power of 2000 mW is frequently used in humans, there was a distinct "pop" sound during laser treatment at this power, which indicated overtreatment of the ciliary body; tissue specimens treated at powers of 1500 to 2000 mW showed structural changes such as ciliary thickening, hemorrhage, and pigment dispersion of the ciliary body. A recent study of MP-CPC in porcine eyes also reported a "pop" sound at 300 J, as well as structural destruction of the pars plicata and ciliary muscles, which is consistent with our findings.[26] Conversely, no evident irreversible tissue degeneration was observed at 250 to 1000 mW; both 500 and 1000 mW significantly lowered IOP, comparable to findings in humans. Therefore we considered these conditions to be suitable for studying the mechanisms of IOP reduction without irreversible tissue degeneration.

We then measured the outflow facility, which is a typical index of conventional outflow (Fig. 1C). Although significant IOP reduction was achieved, outflow facility did not change significantly after MP-CPC. Therefore we presumed that factors other than conventional outflow regulation may be involved in IOP reduction after MP-CPC. However, a few studies have reported that contraction of the longitudinal ciliary muscle occurs after MP-CPC, resulting in deformation of the trabecular meshwork and dilatation of Schlemm's canal. Although our results appear to be contrary to these reports, they do not necessarily negate the conclusions of the previous reports.[17,18,26] Contraction of the ciliary

Investigative Ophthalmology & Visual Science

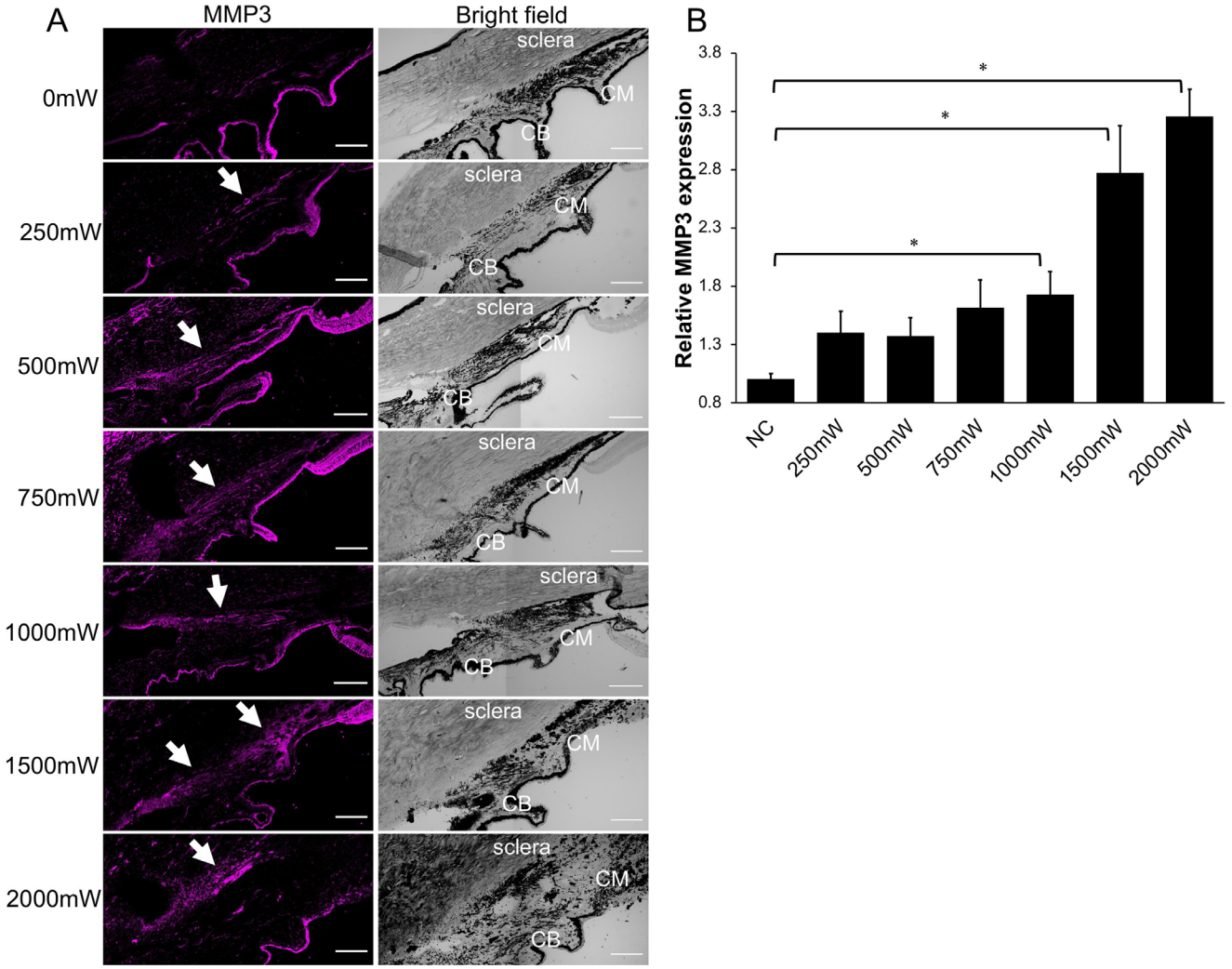

Figure 5. Immunofluorescence staining images and graphs of MMP3 expression patterns. (**A**) The *left panels* show images that were stained with MMP3, the *right panels* show bright field. Significant upregulation of MMP3 was observed in response to increased laser power, localized in the area between the ciliary muscle bundles. The *white arrows* point to areas of MMP3 upregulation. *Scale bar*: 200 µm. (**B**) A graph of the fluorescence intensity of ciliary body. Data are presented as means ± standard errors of the mean (n = 3), Welch's *t* test. $^{*}P < 0.05$, $^{**}P < 0.01$.

muscles may contribute to IOP lowering in a clinical situation, with increased outflow from the conventional pathway. This should be investigated in a clinical scenario; the use of healthy rabbits was a limitation of our experimental design.

We also investigated uveoscleral outflow and demonstrated that it increased after MP-CPC. We used tetramethylrhodamine-labeled dextran, which has served as a tracer for uveoscleral outflow in mice[20]; we visually confirmed that MP-CPC increased uveoscleral outflow in rabbits. Without MP-CPC, tracer signals were observed in the trabecular meshwork but not in the uveoscleral outflow tract. However, tracer signals were observed in the uveoscleral outflow tract after MP-CPC (Fig. 2A). In addition, the tracer signal was observed in a more posterior area of the uveoscleral outflow tract at 1000 than at 500 mW, although the difference was not statistically significant.

Because no morphological changes were observed at laser powers below 1000 mW, we hypothesized that the mechanism for increased uveoscleral outflow under conditions below the threshold of tissue injury might involve proteins that reconstitute the extracellular matrix (e.g., MMPs), as reported for prostaglandins (PGs) in glaucoma.[27,28] Previous studies regarding the relationship between PGs and the permeability of human outflow tissues have reported that PGs produced a time- and concentration-dependent increase in tissue permeability, which increased expression levels of MMP-1, MMP-2, and MMP-3.[29] In a study concerning the effects of PGs in cynomolgus monkeys, an increase in MMPs after PG administration was associated with a decrease in IOP, implying a role for MMPs in IOP reduction.[30] We performed immunofluorescence staining of MMP1–3 and found that their expression levels in the ciliary body increased. Notably, the increase in MMP expression levels coincided with the area of the ciliary muscle bundle known as the uveoscleral outflow tract, implying that increased MMP expression contributed to the increased uveoscleral outflow via extracellular matrix remodeling.

Staining with α-SMA revealed that its expression levels in stromal myofibroblasts and vascular smooth muscles were

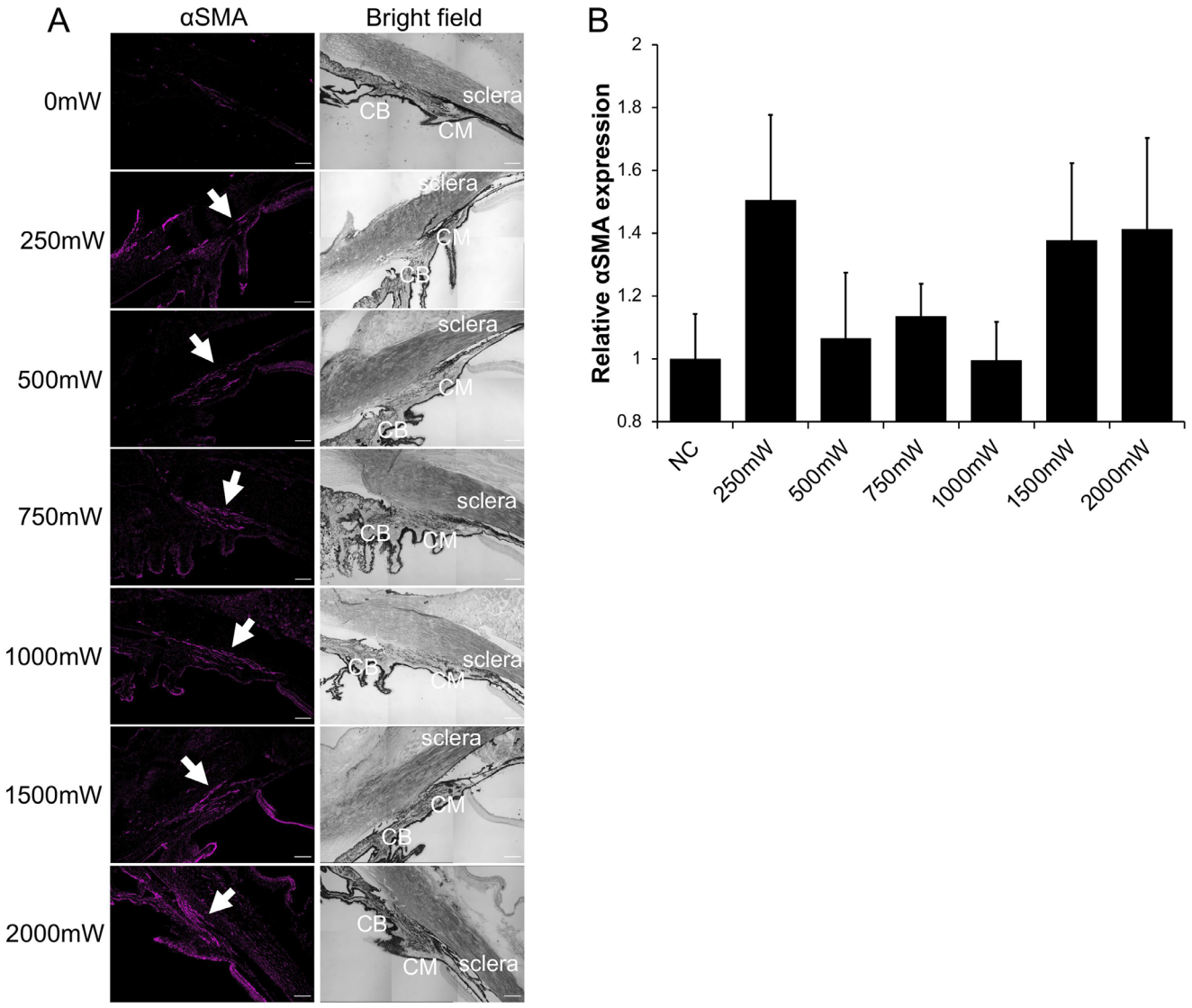

Figure 6. Immunofluorescence staining images and graphs of α-SMA expression patterns. (**A**) The *left panels* show images that were stained with α-SMA, the *right panels* show bright field. Increased α-SMA expression was observed from 250 to 2000 mW, localized in the area between the ciliary muscle bundles. The *white arrows* point to areas of α-SMA upregulation . *Scale bar*: 200 µm. (**B**) A graph of the fluorescence intensity of ciliary body. Although fluorescence intensity increased and the area stained with α-SMA showed broad fluorescence signals beyond the ciliary muscle bundles up to the sclera, the difference was not statistically significant because of large variance between groups. Data are presented as means ± standard errors of the mean (n = 3), Welch's *t* test. $^{*}P < 0.05$, $^{**}P < 0.01$.

upregulated in response to laser treatment at a power of 250 mW; levels tended to increase after MP-CPC, compared to controls, although the differences were not statistically significant. Fibronectin, another fibrosis marker, was markedly upregulated in the ciliary body in response to increased laser power (Fig. 7). Collectively, these results indicate that MP-CPC at lower laser powers may produce a fibrotic response without tissue destruction; higher power may result in tissue destruction and reactive fibrotic changes in the ciliary body. Because of the differences in scleral thickness, anatomy and tissue reactivity between rabbits and humans, it is difficult to determine whether the MP-CPC at certain high power may results in the fibrotic response in actual clinical use in human eyes. However, the reduction of focal fluid production associated with fibrosis may occur, and it is possible that the residual fibrosis may affect drug sensitivity or the results of a second MP-CPC. Further study should be performed in the future to elucidate this consideration.

Because post-MP-CPC conjunctival scarring affects the outcome of filtration surgery, we also investigated the expression patterns of fibrosis markers in the conjunctiva, subconjunctival tissue, and sclera.[31,32] Fibrosis marker levels in subconjunctival tissue increased in response to laser treatment, implying that MP-CPC may cause subconjunctival scarring. Tan et al.[12] previously reported subconjunctival fibrosis after MP-CPC at moderate to high laser powers. Our study differed from that by Tan et al.[12] in terms of the laser powers used and the type of CPC probe, but the results were consistent. Importantly, fibrosis markers also increased at 500 mW, a power much lower than the level used in clinical treatment. In addition, we observed significant upregulation of collagen I in the sclera after MP-CPC. Collectively, it was suggested that MP-CPC may cause fibrosis within

Investigative Ophthalmology & Visual Science

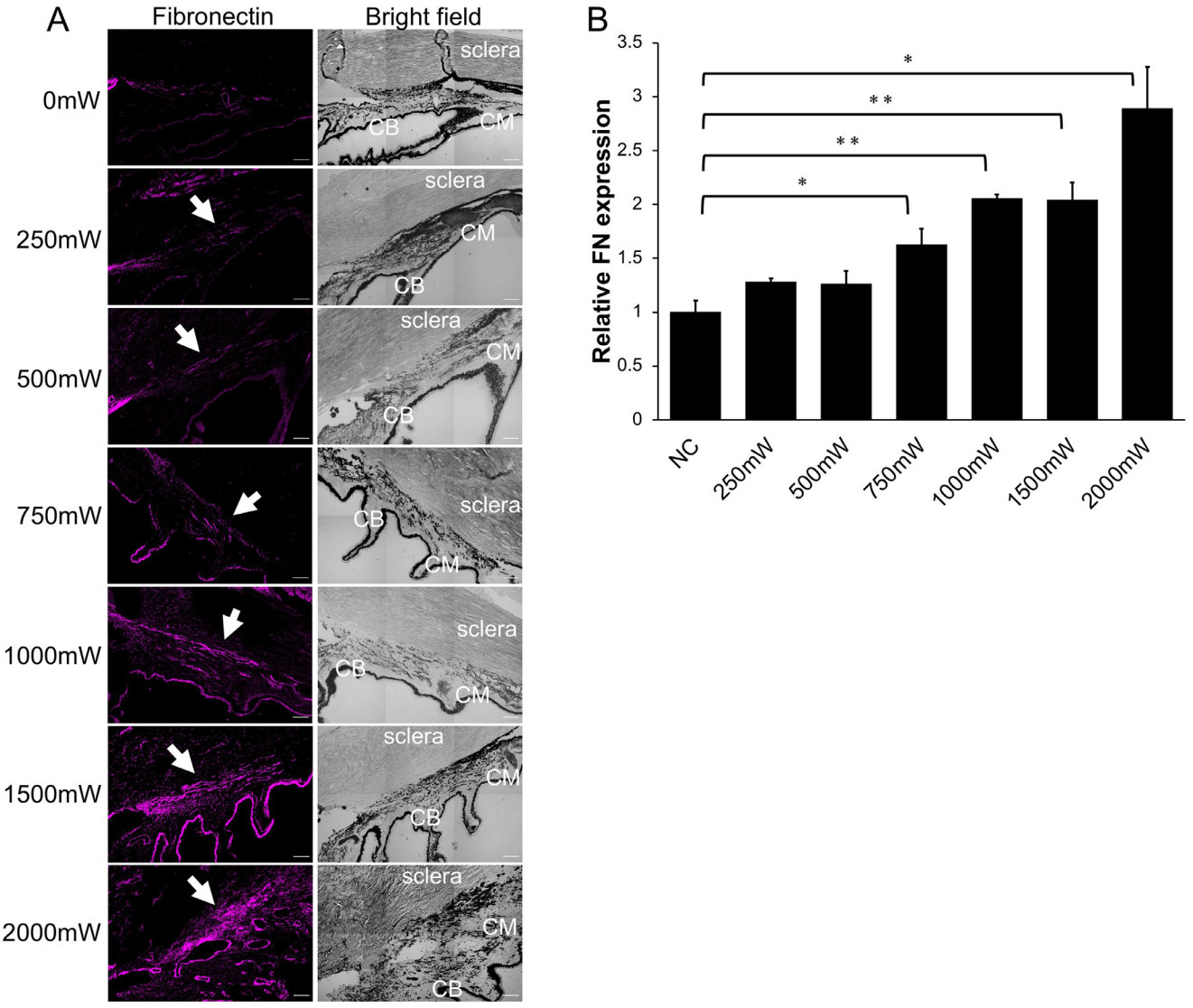

Figure 7. Immunofluorescence staining images and graphs of fibronectin expression patterns. (**A**) The *left panels* show images that were stained with fibronectin, the *right panels* show bright field. Significant upregulation of fibronectin was observed in response to increased laser power, localized in the area between the ciliary muscle bundles. The *white arrows* point to areas of fibronectin upregulation. *Scale bar*: 100 µm. (**B**) A graph of the fluorescence intensity of ciliary body. Data are presented as means ± standard errors of the mean (n = 3), Welch's *t* test. $^{*}P < 0.05$, $^{**}P < 0.01$.

the conjunctiva and sclera even with relatively low power, and additional further study will be needed to clarify this issue.

This study had some limitations. First, it was performed with a small number of animals over a short observation period of one week after MP-CPC. Further studies are needed to investigate the histological reaction more fully over longer time periods. Second, there are some differences in ocular anatomy between rabbits and humans. It has been reported that the proportion of the conventional outflow in the total aqueous humor outflow of rabbits is relatively large compared to that of primates.[33] Eye size and axial length also differ between rabbits and humans, which may have affected the results. Third, this study was performed on healthy rabbits without increased resistance to outflow via the conventional pathway. However, in human clinical practice, MP-CPC is performed on patients with both increased resistance to aqueous humor outflow from the conventional pathway and increased IOP. Therefore the lack of change in outflow facility after MP-CPC in this study does not imply that outflow from the conventional pathway is unaffected in clinical practice. Further studies are needed to determine the effects of MP-CPC on the conventional pathway. Fourth, we could not investigate whether MP-CPC affects aqueous humor production in the present study. Although MP-CPC with the lower power did not cause tissue destruction, it may arise the reactive fibrotic response in the ciliary body especially with the higher power. Therefore it is necessary to further evaluate the effects of MP-CPC on aqueous humor production in the future study.

In conclusion, we found that MP-CPC at low to moderate power levels contributed to IOP reduction by increasing uveoscleral outflow. The underlying mechanisms may involve remodeling of the uveoscleral outflow tract through increased expression of MMPs. Our results support the potential IOP-lowering effects of MP-CPC without tissue

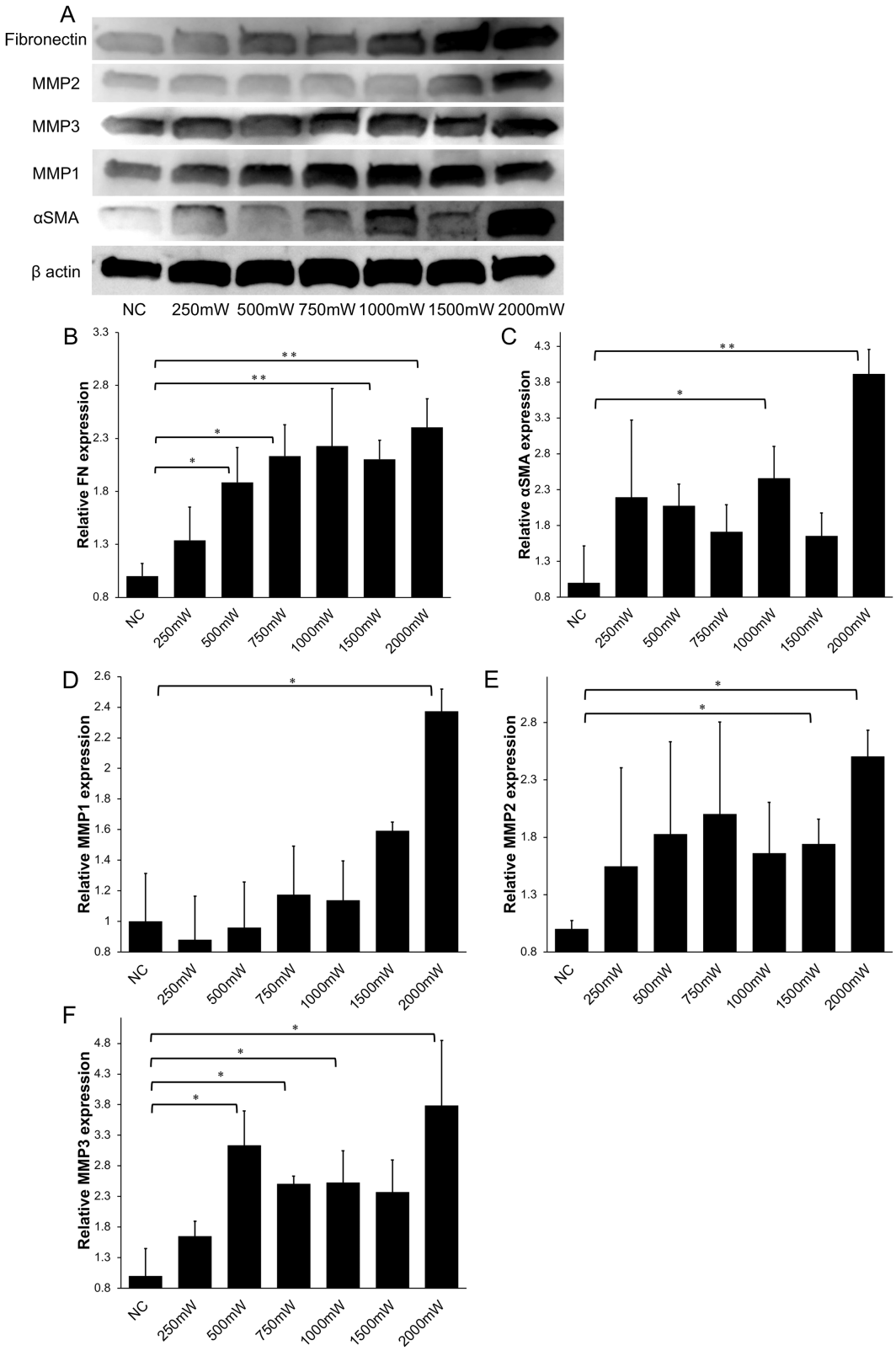

Figure 8. WB of fibronectin, α-SMA, and MMP1-3 in the ciliary body. (**A**) The bands for WB are shown. The expression levels of fibronectin (**B**), α-SMA (**C**), MMP1 (**D**), MMP2 (**E**), and MMP3 (**F**) are shown. Data are presented as means ± standard errors of the mean (n = 3), Welch's *t* test. $^{*}P < 0.05$, $^{**}P < 0.01$.

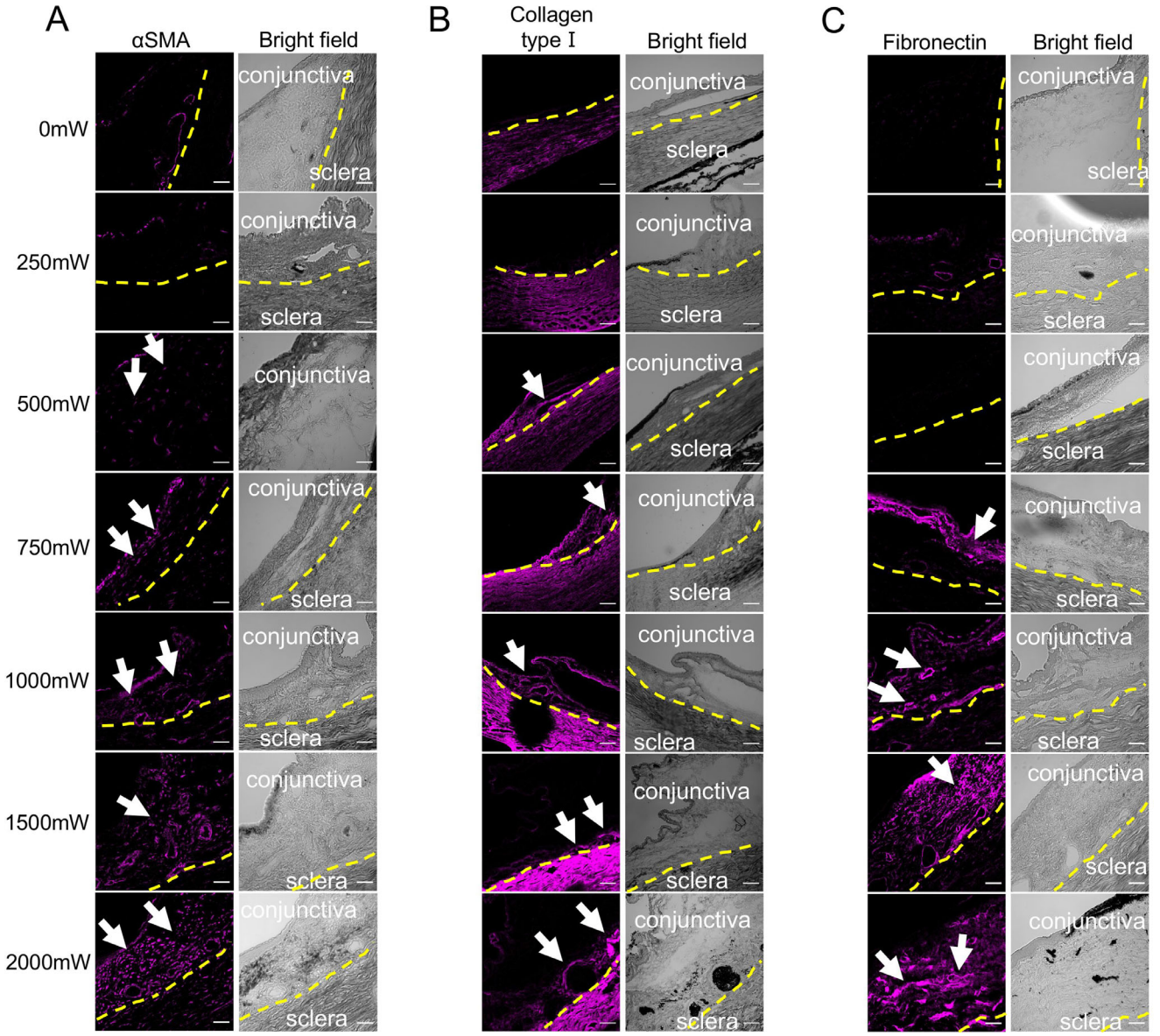

Figure 9. Immunofluorescence staining images of fibrotic markers in the conjunctiva and sclera. (**A, B,** and **C**) The *left panels* show images that were stained with α-SMA, collagen type I, and fibronectin, respectively. The *right panels* show bright field. The signals of α-SMA, collagen type I, and fibronectin increase in response to increasing laser power in the subconjunctival region. The *white arrows* point to areas of fibrotic markers upregulation. The *yellow dashed line* points to the border between conjunctiva and sclera. *Scale bar*: 50 µm.

damage in humans, when using relatively low laser power levels.

Disclosure: **H. Nemoto,** None; **M. Honjo,** None; **M. Okamoto,** Tomey Corporation (E); **K. Sugimoto,** None; **M. Aihara,** None

Acknowledgments

The authors thank the Tomey corporation for the loan of the Cyclo G6 Glaucoma Laser System with the MicroPulse P3 Glaucoma Device and Cycloprobe for use in MP-CPC for research purposes. They are grateful to George Marcellino, PhD, the late Iridex's Vice President, for his generous support from the beginning and giving us the opportunity to start the present study. The English in this document has been checked by at least two professional editors, both native speakers of English.

Supported by the Japan Society for the Promotion of Science (JSPS) grant no. 19K09965 (M.H.) and JSPS KAKENHI grant no. 20H03839 (M.A.).

References

1. Quigley HA, Broman AT. The number of people with glaucoma worldwide in 2010 and 2020. *Br J Ophthalmol*. 2006;90:262–267.
2. Aihara M, Ropo A, Lu F, et al. Intraocular pressure-lowering effect of omidenepag isopropyl in latanoprost non-/low-responder patients with primary open-angle glaucoma or ocular hypertension: the FUJI study. *Jpn J Ophthalmol*. 2020;64(4):398–406.
3. Boland MV, Ervin AM, Friedman DS, et al. Comparative effectiveness of treatments for open-angle glaucoma: a systematic review for the U.S. Preventive Services Task Force. *Ann Intern Med*. 2013;158:271–279.

4. Kwon YH, Fingert JH, Kuehn MH, Alward WLM. Primary open-angle glaucoma. *N Engl J Med*. 2009;360:1113–1124.
5. Weinreb RN, Khaw PT. Primary open-angle glaucoma. *Lancet*. 2004;363(9422):1711–1720.
6. Hennis HL, Stewart WC. Semiconductor diode laser transscleral cyclophotocoagulation in patients with glaucoma. *Am J Ophthalmol*. 1992;113:81–85.
7. Ho CL, Wong EYM, Chew PTK. Effect of diode laser contact transscleral pars plana photocoagulation on intraocular pressure in glaucoma. *Clin Exp Ophthalmol*. 2002;30:343–347.
8. Ramli N, Htoon HM, Ho CL, Aung T, Perera S. Risk factors for hypotony after transscleral diode cyclophotocoagulation. *J Glaucoma*. 2012;21:169–173.
9. Aquino MCD, Barton K, Tan AMWT, et al. Micropulse versus continuous wave transscleral diode cyclophotocoagulation in refractory glaucoma: a randomized exploratory study. *Clin Exp Ophthalmol*. 2015;43:40–46.
10. Tan AM, Chockalingam M, Aquino MC, Lim ZIL, See JLS, Chew PT. Micropulse transscleral diode laser cyclophotocoagulation in the treatment of refractory glaucoma. *Clin Exp Ophthalmol*. 2010;38:266–272.
11. Berger JW. Thermal modelling of micropulsed diode laser retinal photocoagulation. *Lasers Surg Med*. 1997;20:409–415.
12. Tan NYQ, Ang M, Chan ASY, et al. Transscleral cyclophotocoagulation and its histological effects on the conjunctiva. *Sci Rep*. 2019;9(1):18703.
13. Scholz P, Altay L, Fauser S. A review of subthreshold micropulse laser for treatment of macular disorders. *Adv Ther*. 2017;34:1528–1555.
14. Abdelrahman AM, El Sayed YM. Micropulse versus continuous wave transscleral cyclophotocoagulation in refractory pediatric glaucoma. *J Glaucoma*. 2018;27:900–905.
15. Yelenskiy A, Gillette TB, Arosemena A, et al. Patient outcomes following micropulse transscleral cyclophotocoagulation: intermediate-term results. *J Glaucoma*. 2018;27:920–925.
16. Barac R, Vuzitas M, Balta F. Choroidal thickness increase after micropulse transscleral cyclophotocoagulation. *Rom J Ophthalmol*. 2018;62:144–148.
17. Johnstone MA. Microscope real-time video (MRTV), high-resolution OCT (HR-OCT) & histopathology (HP) to assess how transscleral micropulse laser (TML) affects the sclera, ciliary body (CB), muscle (CM), secretory epithelium (CBSE), suprachoroidal space (SCS) & aqueous. *Invest Ophthalmol Vis Sci*. 2019;60:2825.
18. Johnstone MA, Wang RK, Padilla S, Wen K. Transscleral laser induces aqueous outflow pathway motion & reorganization. In: *27th Annual Meeting of the American Glaucoma Society Annual Meeting*. 2017 Mar 2.
19. Barany EH. Simultaneous measurement of changing intraocular pressure and outflow facility in the vervet monkey by constant pressure infusion. *Invest Ophthalmol*. 1964;3:135–143.
20. Lindsey JD, Weinreb RN. Identification of the mouse uveoscleral outflow pathway using fluorescent dextran. *Invest Ophthalmol Vis Sci*. 2002;43:2201–2205.
21. Igarashi N, Honjo M, Aihara M. Effects of mammalian target of rapamycin inhibitors on fibrosis after trabeculectomy. *Exp Eye Res*. 2021;203:108421.
22. Gupta N, Weinreb RN. Diode laser transscleral cyclophotocoagulation. *J Glaucoma*. 1997;6:426–429.
23. Sanchez FG, Peirano-Bonomi JC, Grippo TM. Micropulse Transscleral Cyclophotocoagulation: A Hypothesis for the Ideal Parameters. *Med Hypothesis Discov Innov Ophthalmol*. 2018;7(3):94–100.
24. Liu GJ, Mizukawa A, Okisaka S. Mechanism of intraocular pressure decrease after contact transscleral continuous-wave Nd:YAG laser cyclophotocoagulation. *Ophthalmic Res*. 1994;26:65–79.
25. Tsujisawa T, Ishikawa H, Uga S, et al. Morphological changes and potential mechanisms of intraocular pressure reduction after micropulse transscleral cyclophotocoagulation in rabbits [published online July 31, 2020]. *Ophthalmic Res*, doi:10.1159/000510596.
26. Ahn SM, Choi M, Kim SW, Kim YY. Changes after a month following micropulse cyclophotocoagulation in normal porcine eyes. *Transl Vis Sci Technol*. 2021;10(13):11.
27. Aihara M. Prostanoid receptor agonists for glaucoma treatment. *Jpn J Ophthalmol*. 2021;65(5):581–590.
28. Weinreb RN, Robinson MR, Dibas M, Stamer WD. Matrix metalloproteinases and glaucoma treatment. *J Ocul Pharmacol Ther*. 2020;36:208–228.
29. Kim JW, Lindsey JD, Wang N, Weinreb RN. Increased human scleral permeability with prostaglandin exposure. *Invest Ophthalmol Vis Sci*. 2001;42:1514–1521.
30. Gaton DD, Sagara T, Lindsey JD, Gabelt BT, Kaufman PL, Weinreb RN. Increased matrix metalloproteinases 1, 2, and 3 in the monkey uveoscleral outflow pathway after topical prostaglandin F(2 alpha)-isopropyl ester treatment. *Arch Ophthalmol*. 2001;119:1165–1170.
31. Klink T, Rauch N, Klink J, Grehn F. Influence of conjunctival suture removal on the outcome of trabeculectomy. *Ophthalmologica*. 2009;223:116–123.
32. Landers J, Martin K, Sarkies N, Bourne R, Watson P. A twenty-year follow-up study of trabeculectomy: risk factors and outcomes. *Ophthalmology*. 2012;119:694–702.
33. Johnson M, McLaren JW, Overby DR. Unconventional aqueous humor outflow: a review. *Exp Eye Res*. 2017;158:94–111.
34. Goh Y, Araie M, Nakajima M, Azuma I, Hayaishi O. Effect of topical prostaglandin D2 on the aqueous humor dynamics in rabbits. *Graefes Arch Clin Exp Ophthalmol*. 1989;227:476–481.

Investigative Ophthalmology & Visual Science